



Title	Wave-optical and ray-tracing analysis to establish a compact two-dimensional focusing unit using K-B mirror arrangement
Author(s)	Matsuyama, S.; Mimura, H.; Yamamura, K. et al.
Citation	Proceedings of SPIE – The International Society for Optical Engineering. 2004, 5533, p. 181–191
Version Type	VoR
URL	<a href="https://hdl.handle.net/11094/86988">https://hdl.handle.net/11094/86988</a>
rights	Copyright 2004 Society of Photo-Optical Instrumentation Engineers (SPIE). Downloading of the abstract is permitted for personal use only.
Note	

*The University of Osaka Institutional Knowledge Archive : OUKA*

<https://ir.library.osaka-u.ac.jp/>

The University of Osaka

# Wave-optical and ray-tracing analysis to establish a compact two-dimensional focusing unit using K-B mirror arrangement

S. Matsuyama<sup>a</sup>, H. Mimura<sup>a</sup>, K. Yamamura<sup>b</sup>, H. Yumoto<sup>a</sup>, Y. Sano<sup>a</sup>, K. Endo<sup>b</sup>, Y. Mori<sup>a,b</sup>,  
M. Yabashi<sup>c</sup>, K. Tamasaku<sup>d</sup>, Y. Nishino<sup>d</sup>, T. Ishikawa<sup>c,d</sup>, K. Yamauchi<sup>a</sup>

<sup>a</sup>Department of Precision Science and Technology, Graduate School of Engineering,  
Osaka University, Yamada-oka 2-1, Suita, Osaka 565-0871, Japan

<sup>b</sup>Research Center for Ultra-Precision Science and Technology, Graduate School of Engineering,  
Osaka University, Yamada-oka 2-1, Suita, Osaka 565-0871, Japan

<sup>c</sup>Spring-8/Japan Synchrotron Radiation Research Institute (JASRI),  
Kouto 1-1-1, Mikazuki, Hyogo 679-5148, Japan

<sup>d</sup>Spring-8/RIKEN,  
Kouto 1-1-1, Mikazuki, Hyogo 679-5148, Japan

## 1. ABSTRACT

The spatial resolution of the scanning X-ray microscopy apparently depends on the beam size of the focused X-ray. Recently, highly accurate elliptical mirrors were reported to be fabricated, and nearly diffraction-limited line focusing was achieved. In this study, to realize diffraction-limited and 2-dimensional focusing with such highly accurate mirrors, accuracies to be realized in mirror alignments, for example, adjusting the glancing angle and the in-plane rotation, were estimated by employing two types of simulators. They are appropriately based on geometrical or wave-optical theories. They are alternatively employed according to the degree of accuracy required in the mirror alignment. A focusing unit with the adjusting mechanism fulfilling the required alignment accuracies was constructed, and the relationships between the alignment errors and focused beam profiles were quantitatively examined at the 1km-long beamline (BL29XUL) of Spring-8. Obtained results were in good agreement with the calculated results. Additionally, the alignment accuracy to be realized in the K-B unit equipping mirrors of larger NA (numerical aperture) was calculated to realize sufficient performances in focusing.

Keyword: EEM(elastic emission machining), plasma CVM(chemical vaporization machining), coherent X-rays, hard X-ray focusing, elliptical mirrors, K-B mirror arrangement, X-ray mirror, wave optics, ray trace, X-ray microscopy

## 2. INTRODUCTION

Presently, in total reflection mirror system, ray-trace methods based on geometrical optics were mainly used to evaluate the focused beam properties<sup>1)</sup>. However, in these methods, wavelength is assumed to be infinitely small, so that the focused beam profile in nearly diffraction-limited condition cannot be evaluated. Recently diffraction-limited focusing in hard X-ray mirror optics was reported<sup>2,3)</sup>, and new simulation method based on wave optics<sup>4)</sup> to evaluate the relations between the alignment errors and the focused beam properties are strongly required.

In this study, a simulation code, by which the mirror-alignment accuracy to be realized in K-B mirror arrangement<sup>5)</sup> for hard X-ray focusing can be estimated, was developed. The simulators are based on two theories of geometrical and wave optics according to the degree of the required accuracy. Geometrical optics and wave-optics are employed in estimating the alignment accuracy of the perpendicularity between mirrors and the in-plane rotation, and in estimating one of the glancing angles, respectively.

Results of the calculation shows submicroradian level resolution is required to adjust the glancing angles, so that a flexure hinges and a pulse motor based linear actuators were equipped for the adjusters of glancing angles. Also for the other alignments, designed focusing unit fulfills the estimated requirements.

The developed unit was set at the 1km-long beamline (BL29XUL)<sup>6)</sup> of Spring-8, and the relationships between the alignment errors of two elliptical mirrors and focused beam profiles were investigated two-dimensionally, and the obtained results were in good agreement with the calculated results. Additionally, the required alignment accuracy in another K-B unit having two mirrors of larger NAs (numerical aperture) of  $2.3 \times 10^{-4}$  and  $4.9 \times 10^{-4}$ , which is planned to be development, was estimated to be able to realize nano-scale focusing of hard X-rays.

### 3. Employed optical system with K-B mirrors

To achieve the two-dimensional focusing of hard X-rays at the diffraction-limited condition, the focusing unit, in which a K-B mirror arrangement was employed, was adopted. The configuration of the optical system is shown in Fig. 1. Details of the optical system are shown in Table 1. The surface material of the mirrors is single crystal silicon, and the optics is effective in the X-rays of which photon energy is smaller than 20keV.

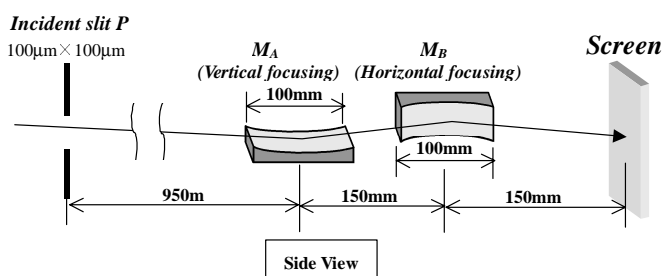


Table 1 Parameters of the elliptical mirrors.

	<b>M<sub>A</sub> mirror</b>	<b>M<sub>B</sub> mirror</b>
<b>Glancing angle</b>	1.40mrad	1.48mrad
<b>Focal length</b>	300mm	150mm
<b>Mirror length</b>	100mm	100mm
<b>Mirror width</b>	5mm	5mm
<b>Length of ellipse</b>	1000.30m	1000.30m
<b>Breadth of ellipse</b>	48.50mm	36.18mm

**Figure 1** Configuration of the optical system. Employed system is fitted to the parameters of the 1km-long beamline (BL29XUL, RIKEN) of Spring-8.

The glancing angles are defined as those at the center of the mirrors. The surface material of the mirror is single crystal silicon, and the optics is effective in the X-rays of which photon energy is smaller than 20keV.

## 4. EVALUATION OF MIRRORS ALIGNMENT ACCURACY USING A RAY TRACE METHOD

### 4.1 Simulation models

In the ray-trace method, the transformations of position vector and the direction cosines of rays by optical devices are calculated on the assumption that wavelength is equal to zero. This method gives many arrival positions on a screen in the relation to the various optical paths. In Fig. 2, an optical system constructed by two elliptical mirrors in a K-B unit, an incident slit and a screen are configured. The position vectors and the direction cosines of rays reflected by the mirror are given by

$$\mathbf{r}_{qk} = \mathbf{r}_{pl} + \mathbf{u}_{pl} \cdot t_{pl} \quad (k=1,2,\dots,N_q), \quad (l=1,2,\dots,N_p)$$

$$\mathbf{u}_{qk} = \mathbf{u}_{pl} - 2 \cdot \mathbf{u}_{pl} \cdot \mathbf{n}_{qk} \quad (k=1,2,\dots,N_q), \quad (l=1,2,\dots,N_p),$$

where  $\mathbf{r}_{pl}$  is a position vector at the point on the virtual light source being the incident slit,  $\mathbf{u}_{pl}$  is a direction cosine of the ray on the light source,  $\mathbf{r}_{qk}$  is a position vector at the intersection point of the ray and the  $M_A$  mirror surface,  $\mathbf{u}_{qk}$  is a direction cosine of the reflected ray on the mirror surface,  $t_{pl}$  is a distance between P and Q, and  $\mathbf{n}_{qk}$  is a normal vector on the  $M_A$  mirror surface. Then, rays between  $M_A$  and  $M_B$  mirrors are given by

$$\mathbf{r}_{rk} = \mathbf{r}_{ql} + \mathbf{u}_{ql} \cdot t_{ql} \quad (k=1,2,\dots,N_r), \quad (l=1,2,\dots,N_q)$$

$$\mathbf{u}_{rk} = \mathbf{u}_{ql} - 2 \cdot \mathbf{u}_{ql} \cdot \mathbf{n}_{rk} \quad (k=1,2,\dots,N_r), \quad (l=1,2,\dots,N_q),$$

where  $\mathbf{r}_{rk}$  is a position vector at the intersection point of the ray and the  $M_B$  mirror surface,  $\mathbf{u}_{rk}$  is a direction cosine by

reflected rays, and  $\mathbf{n}_{rk}$  is a normal vector on the  $M_B$  mirror surface. A position vector  $\mathbf{r}_{sk}$  on the screen is given by  $\mathbf{r}_{sk} = \mathbf{r}_{rl} + \mathbf{u}_{rl} \cdot t_{rl} \quad (k = 1, 2, \dots, N_s), \quad (l = 1, 2, \dots, N_r)$ .

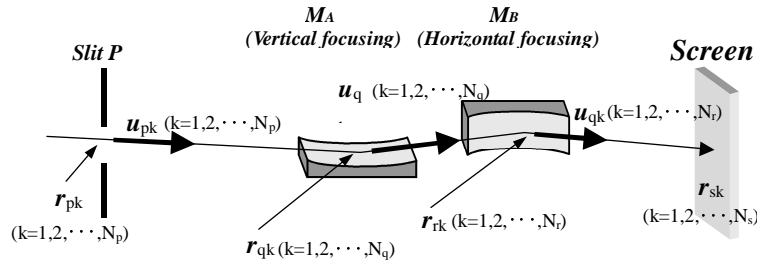


**Figure 2** Optical system constructed by two elliptical mirrors having the K-B type configuration.

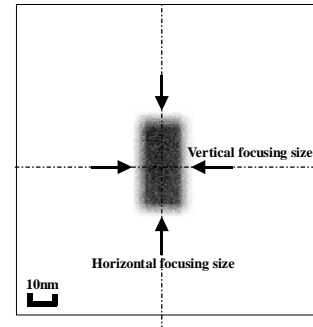


**Figure 3** A typical result of the arrival points of rays on the screen.

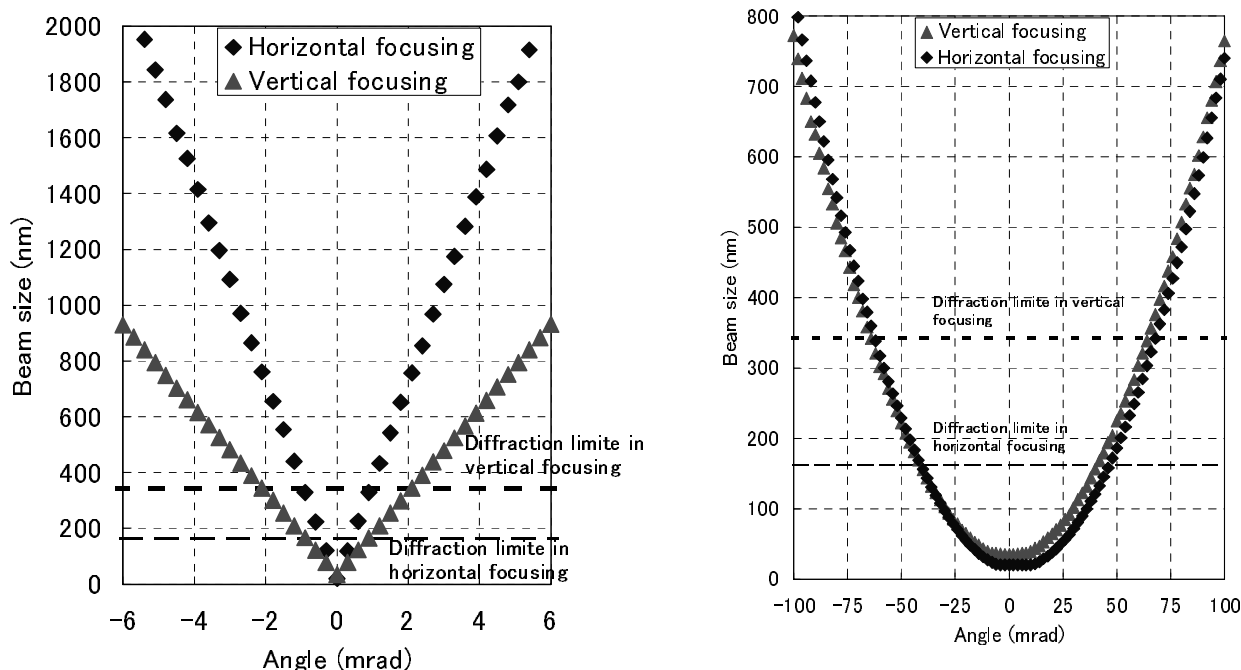
#### 4.2 Simulation results

The relationship between the adjustment error in the perpendicularity of two mirrors and the beam size broadening was investigated. A typical example of the arrival points of rays on the screen is shown in Fig. 3. The beam size is defined in this study as the maximum widths in horizontal and vertical directions. The influence of alignment errors in the perpendicularity between horizontal and vertical mirrors on the beam sizes is shown in Fig. 4. The dotted line indicates a predicted beam size in diffraction-limited focusing. It is given by calculating a Fresnel diffraction pattern based on a rectangle aperture<sup>7)</sup>:

$$d = 2.0 \cdot \lambda \cdot f / D,$$

where  $d$  is the beam size defined as the distance between first minimum,  $f$  is the focal length,  $\lambda$  is the wavelength of the X-ray, and  $D$  is the aperture size of the relevant mirror. As understood from Fig. 4, the acceptable range of the angle error is  $\pm 0.4$  mrad to realize diffraction-limited focusing.

Then, the influence of the alignment errors of in-plane rotation of  $M_A$  and  $M_B$  mirrors on the beam sizes was investigated. Relationship between in-plane rotation error of the  $M_A$  and the beam size in the vertical direction, and relationship between in-plane rotation of the  $M_B$  and that in horizontal direction were evaluated. In Fig. 4, the horizontal and the vertical axes mean in-plane rotation angle of  $M_A$  (or  $M_B$ ) mirror and the beam size, respectively. The dotted line in the graph indicates the predicted beam size in diffraction-limited focusing. To achieve the diffraction-limited focusing, the acceptable ranges of the angle errors in  $M_A$  and  $M_B$  mirrors found to be  $\pm 65$  mrad and  $\pm 40$  mrad, respectively.



(a) Perpendicularity between  $M_A$  and  $M_B$  mirrors.

(b) In-plane rotation errors of  $M_A$  and  $M_B$  mirrors.

**Figure 4** Relationships between the beam sizes and mirror alignment errors of (a) the perpendicularity and (b) in-plane rotation of  $M_A$  and  $M_B$  mirrors. The dotted line in the graph indicates the predicted beam size in diffraction-limited focusing.

## 5. EVALUATION OF MIRRORS ALIGNMENT ACCURACY USING A WAVE OPTICAL SIMULATION

### 5.1 Simulation models

Accuracy higher than that in the former alignments is predicted to be required in aligning glancing angle so that the required alignment accuracy in the glancing is estimated with the wave optical simulator.

Geometrical relationship among the X-ray source, mirrors and screen in the simulator is set as shown in Fig. 5. The principal dimensions employed are those of BL29XUL of SPring-8 so that the incident vertical slit with 100 $\mu$ m width and 100 $\mu$ m height is located 950m upstream of the first mirror (mirror A) center. The distance between the center of the mirror A and the second mirror (mirror B) is 150mm, and the screen is located 150mm downstream of the mirror B. Incident X-ray energy and the glancing angles of the mirror A (B) are set to be 15keV and 1.40mrad (1.48mrad), respectively. In this code, the Fresnel-Kirchhoff integral<sup>7)</sup> is calculated on the following theoretical basis and gives the intensity profile of the totally reflected X-ray beam on the screen.

The complex disturbance at point  $Q$  on the mirror at time  $t$  due to the wave field on the incident slit is given by

$$V(Q, t) = \int_{\text{Slit}} K_1(P, Q) V(P, t - s(P, Q)/c) dP,$$

where  $c$  is the velocity of light, and  $s(P, Q)$  and  $K_1(P, Q)$  are the distance and transmission function from point  $P$  on the incident slit to point  $Q$  on the mirror A, respectively. The complex disturbance at point  $R$  on the mirror B at time  $t$  due to the wave field on the mirror A surface is also given by

$$V(R, t) = \int_{\text{Mirror A}} K_2(Q, R) V(Q, t - s(Q, R)/c) dQ,$$

where  $Q$  is the point on the mirror B and  $K_2(Q, R)$  is different transmission function from the point  $Q$  on the mirror A to point  $R$  on the mirror B. In a similar way, the complex disturbance at the point of  $R$  on the screen is also given by

$$V(S,t) = \int_{\text{MirrorB}} K_3(R,S) V(R,t-s(R,S)/c) dR,$$

Here, point  $S$  on the screen and  $K_3(R,S)$  of another transmission function from the point  $R$  on the mirror B to the point  $S$  on the screen are included. In total reflection, at a glancing angle sufficiently smaller than the critical one, reflectivity at each point on the mirror surface is approximately constant. In addition, phase change originating in an evanescent wave field at each point on the mirror surface is also considered to be constant because the glancing-angle fluctuation is within the order of 0.1mrad in relatively precise mirror surfaces, in which heights of the figure error are around a few nanometers.

The observable X-ray intensity is obtained by averaging in the time scale, as expressed by

$$I(Q) = \langle V(Q,t) V^*(Q,t) \rangle$$

The transversal coherent length of the X-ray at the incident slit of BL29XUL of SPring-8 is about 50 $\mu\text{m}$  in the vertical direction, which means that nearly fully coherent illumination is expected on the surface of the mirror 950m downstream of the slit. This fact gives validity of employing fully coherent Fresnel-Kirchhoff integrals.

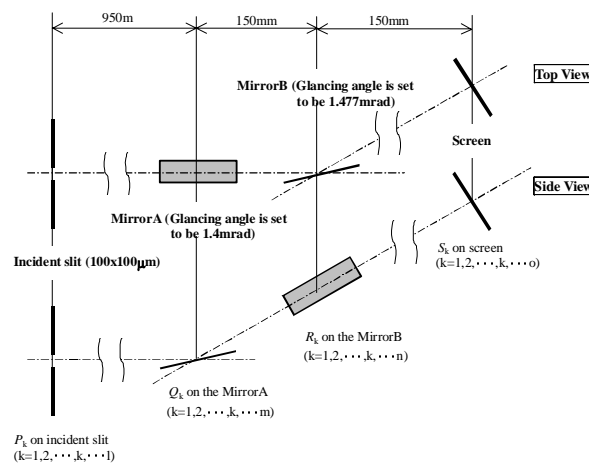
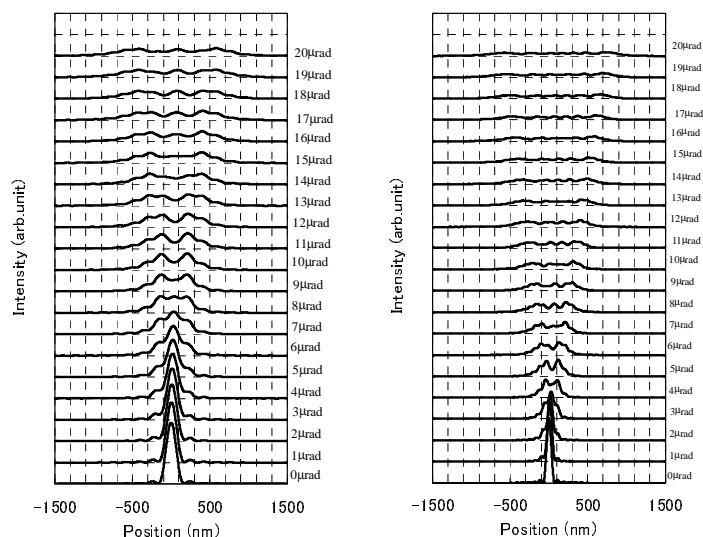


**Figure 5** Employed optical system using K-B mirror arrangement.

## 5.2 Simulation Results

Glancing angle errors were artificially given around the center axis of mirror. Fig. 6 shows the relationship between the errors and focused beam profiles. The beam size shown in Fig.7 is defined as full width at half maximum (FWHM). When the acceptable range is defined to be the error angle, in which the beam size broadening is within 20% of the ideal size, they were  $\pm 7\mu\text{rad}$  and  $\pm 2\mu\text{rad}$  in the vertical and horizontal focusing, respectively.

The displacement from the ideal focal point along the beam axis should be smaller than the focal depth of the optical system. On the assumption that mirror angles are perfectly adjusted, the focused beam profiles were investigated every 1mm along the beam axis near the ideal focal point. As shown in Fig. 10(b), when the range of errors tolerance in the focal length are defined as that in which the beam size broadening is smaller than 20% of the ideal beam size, the acceptable ranges in  $M_A$  and  $M_B$  mirrors are  $\pm 1.2\text{mm}$  and  $\pm 0.2\text{mm}$ , respectively.



(a) Vertical focusing

(b) Horizontal focusing

**Figure 6** The defocusing process: a series of beam profiles at every 1  $\mu\text{rad}$  error from the optimum angle in the X-ray energy of 15 keV.

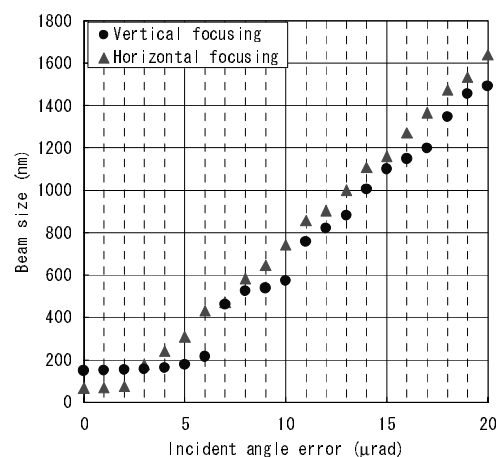


**Figure 7** The relationship between glancing angle errors and focusing beam profiles, where beam size was defined as the FWHM.

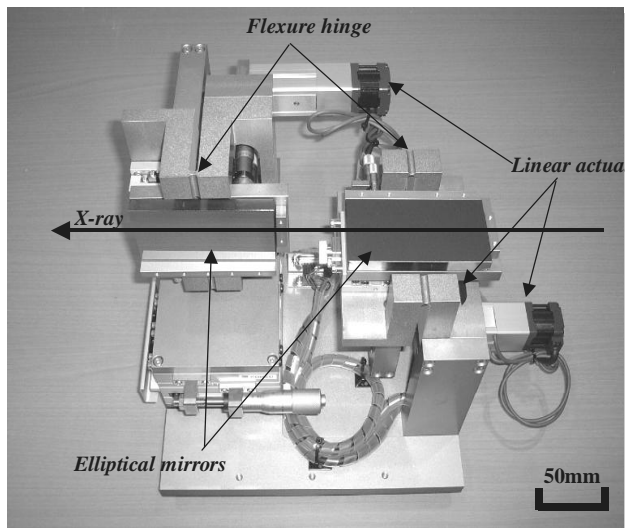
## 6. DEVELOPMENT OF A COMPACT TWO-DIMENSIONAL FOCUSING UNIT USING K-B MIRROR ARRANGEMENT

Estimated accuracies to be realized in mirror alignments were summarized in Table 2. An X-ray focusing unit fulfilling these accuracy criteria was designed and actually constructed. The schematic view of the unit is shown in Fig. 8. The glancing angle adjustment requires the highest accuracy against the other alignment parameters so that the flexure hinge and the pulse motor based linear actuator having sufficient feed resolution were employed in the glancing angle adjuster. The employed mechanism can adjust the angles without any mechanical sliding and friction. The angular resolutions realized in the unit were 1  $\mu\text{rad}$  both in  $M_A$  and  $M_B$  mirrors. The adjuster for the perpendicularity between these mirrors is consisted of two linear actuators located under the vertical focusing mirror, and has the angular resolution of 0.2 mrad. In the adjuster of the in-plane rotation, just a micrometer head is employed because the acceptable range of alignment error is  $\pm 50$  mrad.

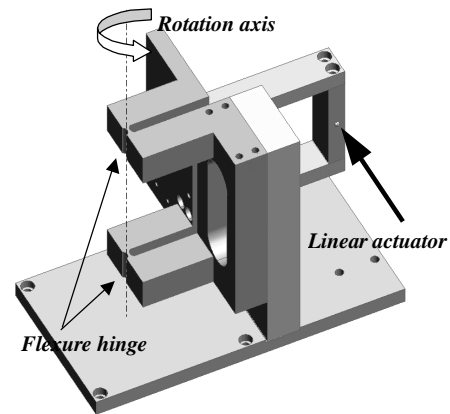
To minimize the elastic deformation of the mirrors by gravitational force, the mirrors are placed on the mirror stages using three support balls arranged at the Airy points. The elastic deformation distribution of the mirror on the three support balls was simulated using a finite element method, and the maximum deformation of less than 1 nm was confirmed.

**Table 2** Summary of acceptable range of mirrors alignment to realize diffraction-limited focusing two-dimensionally in X-ray energy of 15 keV.

	Glancing angle	Perpendicularity	In-plane rotation	Focal length
<b>Mirror A</b>	$\pm 7 \mu\text{mrad}$	$\pm 0.4 \text{ mrad}$	$\pm 65 \text{ mrad}$	$\pm 1.2 \text{ mm}$
<b>Mirror B</b>	$\pm 2 \mu\text{rad}$		$\pm 40 \text{ mrad}$	$\pm 0.2 \text{ mm}$



(a) Photograph of the focusing unit.



(b) Schematic drawing of the glancing angle adjuster.

**Figure 8** Schematic views of the K-B focusing unit.

## 7. EXPERIMENTS OF TWO-DIMENSIONAL FOCUSING

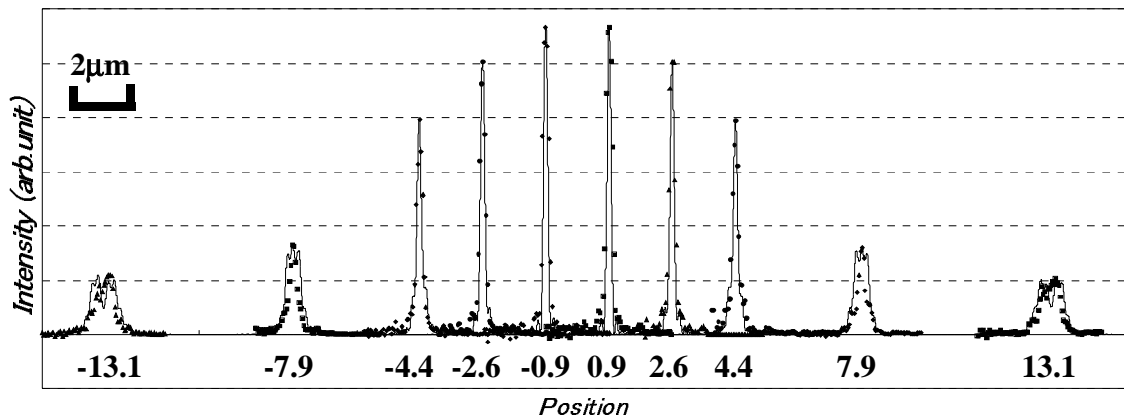
The developed K-B focusing unit equipping ultraprecisely fabricated mirrors<sup>8)~11)</sup> by EEM<sup>12)~14)</sup> and P-CVM<sup>15)~17)</sup> were installed into the 1km-long beamline (BL29XUL, RIKEN), and two-dimensional focusing performance was tested, with the X-ray energy of 15keV, and the way to measure the beam profiles was a wire scan method using a gold wire with the diameter of 200 $\mu$ m. The perpendicularity between two mirrors and the in-plane rotation angle were adjusted within acceptable range.

Figure 9 shows the tuning process of the glancing angle of the  $M_A$  mirror as a series of beam profiles. The subscripts at the bottom of the graph correspond to the errors (in  $10^{-6}$  radian) from the optimum glancing angle. The calculated beam profiles are shown in the same graph with the solid lines together with the measured profiles shown with dots. As understood from the figure, the measured results were in good agreement with the calculated ones.

Figure 10 shows the cross-sectional intensity profiles measured every 1mm in the beam direction over the  $\pm 5$ mm range from the focal point. The subscripts correspond to the displacement of the wire from the optimum focal position. The measured results agreed well with the calculated ones.

After the adjustments of the glancing angle and the focal length, the two-dimensionally focused beam profiles were measured in the X-ray energy of 15keV, and the results were shown in Fig. 11. The beam size of 180nm(V) x 90nm(H) in FWHM was seen to be achieved. Additionally, the beam profile calculated by using the measured mirror profile under the optimum mirror-alignment condition was presented as a solid line in Fig. 11. The obtained results are seen to be well consistent with the calculated results.





**Figure 9** Tuning process of the glancing angle of  $M_A$  mirror as a series of beam profiles. Measured and wave-optically calculated profiles are shown with the dots and the solid lines, respectively.

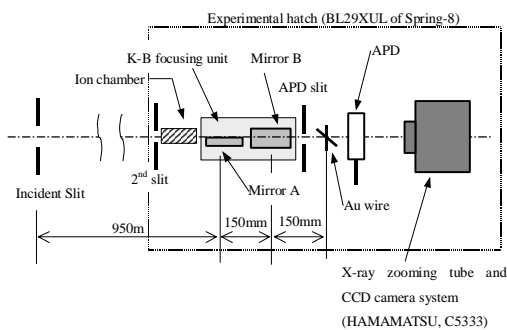
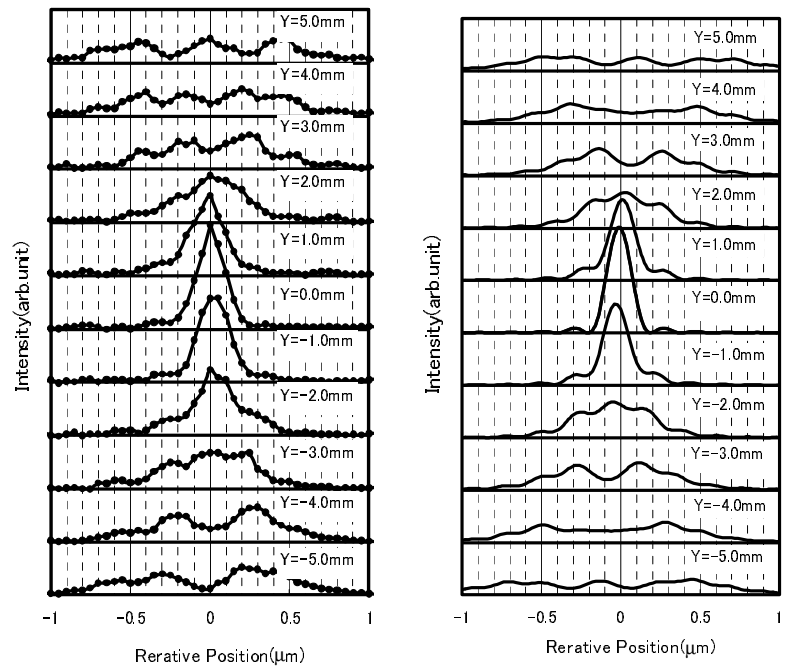


**Figure 8** Schematic view of the experimental configuration. A wire scanning method with a gold wire of  $200\mu\text{m}$  diameter was employed. An avalanche photodiode detector (APD)<sup>18,19</sup> for measuring the beam intensity and an ion chamber to measure the incident beam intensity are installed.



(a) Measured profiles

(b) Calculated profiles

**Figure 10** Cross-sectional intensity profiles measured every 1mm in the beam direction over the 5mm range from the focal plane and calculated on wave optical basis.

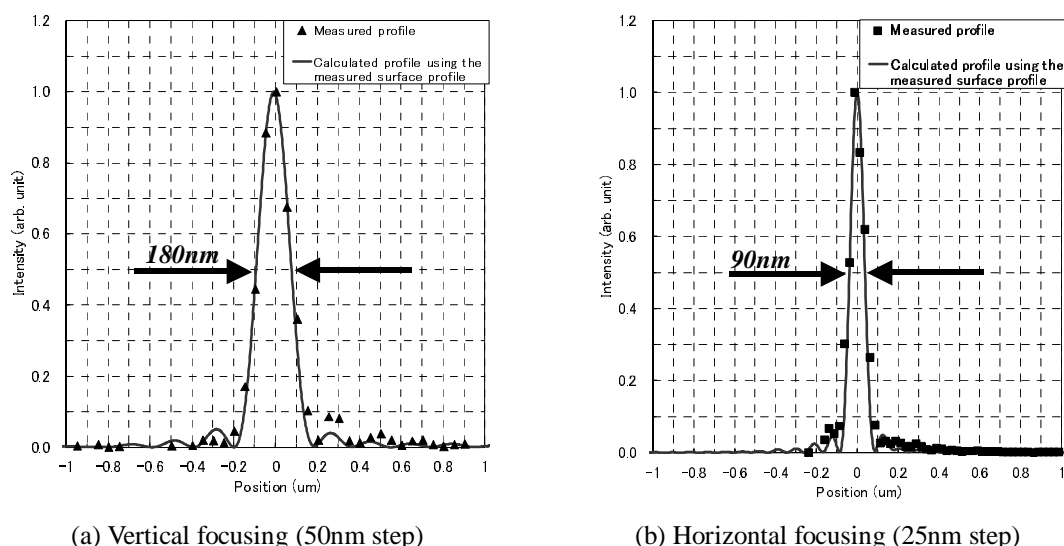


**Figure 11** Two-dimensional intensity profile experimentally obtained in the X-ray energy of 15keV

## 8. ESTIMATING THE REQUIRED ALIGNMENT ACCURACY OF MIRRORS HAVING LARGE NA (NUMERICAL APERTURE)

In the scanning X-ray microscopy, higher-resolution can be realized with smaller probe beam. Currently, large NA elliptical mirrors having platinum or multi layer coating are going to be fabricated. In our group, mirror figures having large NA are newly designed. Installation into the BL19LXU<sup>20)</sup> of SPring-8, which has a 27m-long undulator and realizes the highest X-ray intensity, was considered in the optical design. Intensity of the focused X-ray is estimated roughly 3800 times brighter than the former focusing unit. In this estimation, the undulator brightness, the NA of mirrors and the beam broadening at the experimental hatch are taken into account. Parameters of the newly designed elliptical mirrors are shown in Table 3. The acceptable alignment errors estimated, to realize two-dimensional diffraction-limited focusing, are summarized in Table 4. X-ray energy is 15keV in the estimation. The adjusting accuracy to be required in the system is understood to be much higher than that in the former system. New mirrors and the aligner are under development, now.

**Table 3** Parameters of newly designed elliptical mirrors

	<b>M<sub>H</sub> mirror</b>	<b>M<sub>V</sub> mirror</b>
<b>Glancing angle</b>	4.00mrad	3.65mrad
<b>Focal length</b>	252mm	150mm
<b>Mirror length</b>	100mm	100mm
<b>Mirror width</b>	5mm	5mm
<b>Length of ellipse</b>	33.53m	33.53m
<b>Breadth of ellipse</b>	16.41mm	11.56mm

**Table 4** Summary of acceptable ranges of alignments to realize two-dimensional diffraction-limited focusing in X-ray energy of 15keV.

	Glancing angle	Perpendicularity	In-plane rotation	Focal length
<b>Mirror H</b>	$\pm 1.5\mu\text{rad}$	$\pm 0.1\text{mrad}$	$\pm 19\text{mrad}$	$\pm 0.1\text{mm}$
<b>Mirror V</b>	$\pm 0.9\mu\text{rad}$		$\pm 20\text{mrad}$	$\pm 0.04\text{mm}$

## 9. CONCLUSION

We estimated the acceptable alignment error in the K-B focusing unit of hard X-rays to realize diffraction-limited focusing using optical simulators based on geometrical and/or wave-optical theories. An X-ray focusing unit fulfilling the required alignment accuracies estimated by the simulators was designed and developed. It was installed into the 1km-long beamline (BL29XUL) of Spring-8, and the relationships between the alignment errors and focused beam profiles were investigated. Experimentally obtained results were in good agreement with the calculated results.

Additionally, the alignment accuracy to be satisfied in the larger NA mirror system was estimated. The new mirror system was clarified to require higher degree of accuracy than the former one, e.g. the acceptable range of  $\pm 0.9\mu\text{rad}$  in the glancing angle adjusting. The focusing unit fulfilling the requirements is under development. The larger NA mirror system will make it possible to realize nanofocusing of hard X-rays.

## ACKNOWLEDGEMENT

This research was partially supported by Grant-in-Aid for Scientific Research (S), 15106003, 2004 and 21<sup>st</sup> Century COE Research, Center for Atomistic Fabrication Technology, 2004 from the Ministry of Education, Sports, Culture, Science and Technology.

## REFERENCES

- [1] P. Naulleau, K. Goldberg, P. Batson, S. Jeong and J. Underwood: *Appl. Opt.* **40**, 3703 (2001).
- [2] K. Yamauchi, K. Yamamura, H. Mimura, Y. Sano, A. Saito, A. Souvorov, M. Yabashi, K. Tamasaku, T. Ishikawa and Y. Mori: *J. Synchrotron rad.* **9**, 313 (2002).
- [3] K. Yamauchi, K. Yamamura, H. Mimura, Y. Sano, A. Saito, K. Endo, A. Souvorov, M. Yabashi, K. Tamasaku, T. Ishikawa and Y. Mori: *Jpn. J. Appl. Phys.* **42**, 7129 (2003).
- [4] K. Yamauchi, K. Yamamura, H. Mimura, Y. Sano, A. Saito, M. Kanaoka, K. Endo, A. Souvorov, M. Yabashi, K. Tamasaku, T. Ishikawa and Y. Mori: *Proc. SPIE* **4782**, 271 (2002).
- [5] P. Kirkpatrick and A. V. Baez: *J. Opt. Soc. Am.* **38**, 766 (1948).
- [6] T. Ishikawa, K. Tamasaku, M. Yabashi, S. Goto, Y. Tanaka, H. Yamazaki, K. Takeshita, H. Kimura, H. Ohashi, T. Matsushita and T. Ohata: *Proc. SPIE* **4154**, 1 (2001).
- [7] M. Born and E. Wolf, *Principles of Optics*, 6<sup>th</sup> edition, Cambridge University Press (1997).
- [8] K. Yamamura, H. Mimura, K. Yamauchi, Y. Sano, A. Saito, T. Kinoshita, K. Endo, A. Souvorov, M. Yabashi, K. Tamasaku, T. Ishikawa and Y. Mori: *Proc. SPIE* **4782**, 265 (2002).
- [9] K. Yamauchi, K. Yamamura, H. Mimura, Y. Sano, A. Saito, K. Ueno, K. Endo, A. Souvorov, M. Yabashi, K. Tamasaku, T. Ishikawa, and Y. Mori: *Rev. Sci. Instrum.* **74**, 2894 (2003).
- [10] Y. Mori, K. Yamauchi, K. Yamamura, H. Mimura, A. Saito, Y. Sano, K. Endo, A. Souvorov, M. Yabashi, K. Tamasaku and T. Ishikawa M. Shimura, Y. Ishizaka: *Proc. SPIE* **5193**, 11 (2003).
- [11] Y. Mori, K. Yamauchi, K. Yamamura, H. Mimura, Y. Sano, A. Saito, K. Ueno, K. Endo, A. Souvorov, M. Yabashi, K. Tamasaku and T. Ishikawa: *Proc. SPIE* **5193**, 105 (2003).
- [12] Y. Mori, K. Yamauchi and K. Endo: *Precis. Eng.* **9**, 123 (1987).
- [13] Y. Mori, K. Yamauchi and K. Endo: *Precis. Eng.* **10**, 24 (1988).
- [14] K. Yamauchi, H. Mimura, K. Inagaki and Y. Mori: *Rev. Sci. Instrum.* **73**, 111 (2002).
- [15] Y. Mori, K. Yamamura and Y. Sano: *Rev. Sci. Instrum.* **71**, 4620 (2000).
- [16] Y. Mori, K. Yamauchi, K. Yamamura and Y. Sano: *Rev. Sci. Instrum.* **71**, 4627 (2000).
- [17] K. Yamamura, K. Yamauchi, H. Mimura, Y. Sano, A. Saito, K. Endo, A. Souvorov, M. Yabashi, K. Tamasaku, T. Ishikawa and Y. Mori: *Rev. Sci. Instrum.* **74**, 4549 (2003).
- [18] S. Kishimoto: *Rev. Sci. Instrum.* **63**, 824 (1992).

- [19] Q. R. Baron and S. L. Ruby: *Nucl. Instrum. Methods A* **343**, 517 (1994).
- [20] T. Hara, M. Yabashi, T. Tanaka, T. Bizen, S. Goto, X. M. Maréchal, T. Seike, K. Tamasaku, T. Ishikawa, and H. Kitamura: *Rev. Sci. Instrum.* **73**, 1125 (2002).